Diminished Superoxide Generation Is Associated With Respiratory Chain Dysfunction and Changes in the Mitochondrial Proteome of Sensory Neurons From Diabetic Rats

Eli Akude,[1,2] Elena Zherebitskaya,[1] Subir K. Roy Chowdhury,[1] Darrell R. Smith,[1,2] Rick T. Dobrowsky,[3] and Paul Fernyhough[1,2]

OBJECTIVE—Impairments in mitochondrial function have been proposed to play a role in the etiology of diabetic sensory neuropathy. We tested the hypothesis that mitochondrial dysfunction in axons of sensory neurons in type 1 diabetes is due to abnormal activity of the respiratory chain and an altered mitochondrial proteome.

RESEARCH DESIGN AND METHODS—Proteomic analysis using stable isotope labeling with amino acids in cell culture (SILAC) determined expression of proteins in mitochondria from dorsal root ganglia (DRG) of control, 22-week-old streptozotocin (STZ)-diabetic rats, and diabetic rats treated with insulin. Rates of oxygen consumption and complex activities in mitochondria from DRG were measured. Fluorescence imaging of axons of cultured sensory neurons determined the effect of diabetes on mitochondrial polarization status, oxidative stress, and mitochondrial matrix-specific reactive oxygen species (ROS).

RESULTS—Proteins associated with mitochondrial dysfunction, oxidative phosphorylation, ubiquinone biosynthesis, and the citric acid cycle were downregulated in diabetic samples. For example, cytochrome *c* oxidase subunit IV (COX IV; a complex IV protein) and NADH dehydrogenase Fe-S protein 3 (NDUFS3; a complex I protein) were reduced by 29 and 36% ($P < 0.05$), respectively, in diabetes and confirmed previous Western blot studies. Respiration and mitochondrial complex activity was significantly decreased by 15 to 32% compared with control. The axons of diabetic neurons exhibited oxidative stress and depolarized mitochondria, an aberrant adaption to oligomycin-induced mitochondrial membrane hyperpolarization, but reduced levels of intramitochondrial superoxide compared with control.

CONCLUSIONS—Abnormal mitochondrial function correlated with a downregulation of mitochondrial proteins, with components of the respiratory chain targeted in lumbar DRG in diabetes. The reduced activity of the respiratory chain was associated with diminished superoxide generation within the mitochondrial matrix and did not contribute to oxidative stress in axons of diabetic neurons. Alternative pathways involving polyol pathway activity appear to contribute to raised ROS in axons of diabetic neurons under high glucose concentration. ***Diabetes*** **60:288–297, 2011**

Enhanced oxidative stress is thought to be a central pathologic feature in the etiology of diabetic peripheral neuropathy (1). To develop more targeted therapeutics toward ameliorating oxidative stress and the development of diabetic peripheral neuropathy, considerable effort has focused on identifying the cellular source of reactive oxygen species (ROS) over the past decade. Brownlee et al. (2) suggested that mitochondrial superoxide generation may be a critical feature in the onset of diabetic complications. In cultured endothelial cells, hyperglycemia induced excessive electron flux through the respiratory chain that promoted mitochondrial hyperpolarization and elevated ROS production (2,3). These investigators proposed that hyperglycemia increases mitochondrial NADH levels and that increased electron availability and/or saturation causes partial reduction of oxygen to superoxide in the proximal part of the respiratory chain (2). In support of this mechanism, epineurial arterioles serving the sciatic nerve of STZ-diabetic rats show increased levels of mitochondrial superoxide that is dependent on complex I activity (4). On the other hand, studies in diabetic retina suggest that metabolism of high glucose concentrations does not operate in a fashion that supports superoxide formation by the respiratory chain (5). Similarly, in sensory neurons from STZ-diabetic rats, the mitochondrial membrane potential is depolarized and not hyperpolarized, as observed in endothelial cells exposed to hyperglycemia (6,7). Further, lumbar dorsal root ganglia (DRG) from diabetic rats exhibit reduced respiratory chain activity that correlate with the downregulation of select proteins within the electron transport chain complexes (8). These findings are aligned with studies in diabetic heart where mitochondrial respiration and enzymatic activities are reduced (9,10). In addition, activities of citrate synthase and mitochondrial respiratory chain are decreased in the skeletal muscle of patients with type 2 diabetes (11–13).

Therefore, production of mitochondrial superoxide may exhibit fundamental differences in cells that are targets of diabetic complications. Indeed, the tissue-specific nature of mitochondrial remodeling in diabetes is directly underscored by results from an unbiased proteomic study that identified a differential effect of diabetes on the mitochondrial protein expression and oxidative capacity. For exam-

From the [1]St. Boniface Hospital Research Centre, Winnipeg, Manitoba, Canada; the [2]Department of Pharmacology and Therapeutics, University of Manitoba, Winnipeg, Manitoba, Canada; and the [3]Department of Pharmacology and Toxicology, University of Kansas, Lawrence, Kansas.
Corresponding author: Paul Fernyhough, paulfernyhough@yahoo.com.
Received 10 June 2010 and accepted 20 September 2010. Published ahead of print at http://diabetes.diabetesjournals.org on 28 September 2010. DOI: 10.2337/db10-0818.
E.A. and E.Z. contributed equally to this study.
R.T.D. and P.F. contributed equally to this study.

ple, proteins associated with oxidative phosphorylation were more depressed and respiratory activity decreased in heart compared with liver mitochondria from diabetic Akita mice (14). Since DRG sensory neurons are highly susceptible to glucotoxicity (15), we examined the effect of diabetes on the mitochondrial proteome, respiratory capacity, and superoxide production. Our previous work on sensory neurons in diabetes demonstrated mitochondrial depolarization within the perikarya and lowered respiratory chain capacity (6,8); however, our objective in the current work was to relate the effects of diabetes on mitochondrial proteome expression to mitochondrial physiology and function within the axon where oxidative stress and degeneration are most clearly defined (16–18). To this end, we exploited the use of stable isotope labeling of cells in culture (SILAC) (19) to provide a set of culture-derived isotope tags (20) to serve as internal standards for a quantitative proteomic analysis. We demonstrate that in diabetes impaired respiratory chain function correlates with decreased protein expression, and in mitochondria of axons, these deficits are associated with membrane depolarization and reduced respiratory chain-derived ROS generation. These data support the conclusion that glucose-dependent superoxide production within the mitochondrial matrix is not a major contributor to oxidative stress in axons of DRG in long-term diabetes.

RESEARCH DESIGN AND METHODS

Induction, treatment, and confirmation of type 1 diabetes. Male Sprague Dawley rats were made diabetic with a single intraperitoneal injection of 75 mg/kg STZ (Sigma, St Louis, MO). Insulin implants (two Linplant implants; Linshin Canada, Toronto, ON, Canada) were placed subcutaneously into STZ-diabetic rats after 18 weeks of diabetes and kept in place for 4 weeks. Animals were killed and tissue collected after 22 weeks of diabetes. Animal procedures followed the guidelines of the University of Manitoba Animal Care Committee using the Canadian Council of Animal Care rules.

Preparation of isolated mitochondria from DRG and isotopically labeled SC16 cells. Mitochondrial preparations from DRG were isolated as described (8,21). Immortalized SC16 Schwann cells were cultured in low glucose Dulbecco's modified Eagle's medium containing 125 mg/l $^{13}C_6$-lysine (K6) and 84 mg/l $^{13}C_6$,$^{15}N_4$-arginine (R10) (Cambridge Isotopes, Andover, MA), 10% dialyzed FCS (Atlas Biologicals, Fort Collins, CO), and antibiotics (22). Crude mitochondria from labeled cells were obtained by differential centrifugation and purified through a discontinuous Nycodenz gradient (23). For quantitative analysis of the DRG mitochondrial proteome, the K6R10-labeled mitochondria were used as a source of culture-derived isotope tags to serve as internal standards (20). After assessing the protein concentration of the preparations, the unlabeled mitochondrial protein (K0R0) obtained from each of the control ($n = 4$), diabetic ($n = 3$), and diabetic + insulin ($n = 4$) treatments were mixed in a 2:1 ratio with K6R10 labeled mitochondria. Total protein (60–70 μg) was subjected to SDS-PAGE, the gel was stained with colloidal Coomassie blue, and lanes were cut into 5 × 1 cm pieces.

RP-HPLC/LTQ-FT MS/MS and protein identification and quantification criteria. A detailed description of these parameters is provided in supplementary Table 1 in the online appendix 2 at http://diabetes.diabetesjournals.org/cgi/content/full/db10-0818/DC1. See Fig. 1 for an overview of the SILAC approach.

Adult rat DRG sensory neuron culture. Lumbar DRG sensory neurons from adult male Sprague-Dawley rats were isolated and dissociated as described (6,16). Rats were either age-matched control or 22-week STZ-diabetic. Cells were plated onto poly-D-L-ornithine hydrobromide and laminin-coated 25-mm glass cover slips (German glass #1, Electron Microscopy Sciences, Hatfield, PA). Neurons were grown in defined Hams F-12 medium with N2 additives (no insulin), supplemented with neurotrophic factors: 0.1 ng/ml nerve growth factor, 1.0 ng/ml glial cell line-derived neurotrophic factor, and 0.1 ng/ml neurotrophin-3 (all obtained from Sigma). Neurons from control rats were cultured with 10 mmol/l D-glucose and 10 nmol/l insulin and neurons from diabetic rats were plated with 25 mmol/l D-glucose and no insulin for 1 to 3 days.

Determination of oxidative stress in axons. Cultured neurons from control or diabetic rats were either *1*) imaged in real time for intracellular ROS by loading with 1.2 μmol/l 5-(and-6)-chloromethyl-2′7′-dichlorodihydrofluorescein diacetate acetyl ester (CM-H_2DCFDA, or *2*) fixed and stained for adducts of 4-hydroxy-2-nonenal (4-HNE) (a product of lipid peroxidation), as previously described (16). To study the role of polyol pathway in ROS production, cultures were treated acutely with the specific sorbitol dehydrogenase (SDH) inhibitor, SDI-158 (24) (10 μmol/l; a gift from Dr. Nigel Calcutt, University of California San Diego).

Assessment of mitochondrial membrane potential in cultured neurons. Cultured DRG neurons were loaded with 3.0 nmol/l tetramethyl rhodamine methyl ester (TMRM; Molecular Probes, Eugene, OR) for 1 h and the fluorescence signal in the axons detected with a Carl Zeiss LSM510 confocal inverted microscope (X100 objective; excitation at 540 nm and emission >560 nm). The TMRM was used in subquench mode—in which decreased fluorescence intensity indicates reduced mitochondrial inner membrane potential (25). Antimycin A and oligomycin (Sigma) were injected into the culture media to a final concentration of 10 μmol/l and 1 μmol/l, respectively, at 1 min after baseline fluorescence measurements. All axons in each field were assessed as the average of fluorescence pixel intensity per axon length using the Carl Zeiss software package (16).

Intramitochondrial ROS measurement. Intramitochondrial ROS generation, mainly superoxide, was detected using the fluorescent MitoSOX red dye (Molecular Probes, catalog #M36008). Lumbar DRG neurons were loaded with 400 nmol/l of MitoSOX red (in 100% anhydrous DMSO; Molecular Probes) for 15 min with or without 1.0 μmol/l oligomycin at 37°C, and then washed three times with F-12 and excited at 514 nm and emission >560 nm.

Respiratory chain function. Oxygen consumption was determined at 37°C using the OROBOROS Oxygraph-2K (OROBOROS Instruments GmbH, Innsbruck, Austria) (8). Mitochondria from freshly isolated and intact lumbar DRG were resuspended in KCl medium (80 mmol/l KCl, 10 mmol/l Tris-HCl, 3.0 mmol/l $MgCl_2$, 1.0 mmol/l EDTA, 5.0 mmol/l potassium phosphate, pH 7.4). Various substrates and inhibitors of the mitochondrial respiratory chain complexes were used as described (8). Enzymatic activities in lumbar DRG mitochondrial preparations were performed spectrophotometrically as previously described (8).

Statistical analysis. When appropriate, data were subjected to one-way ANOVA with post hoc comparison using the Tukey test or regression analysis with a one-phase exponential decay parametric test with the Fisher parameter (GraphPad Prism 4, GraphPad Software, San Diego, CA). In all other cases, two-tailed Student t tests were performed. To determine the threshold for statistical significance for the proteomic data, proteins showing at least a 20 or 25% increase or decrease were grouped and compared with the entire dataset using a Kruskal-Wallis nonparametric ANOVA and the Dunn multiple comparison test. This analysis indicated that a minimum difference of 25% was necessary for a value to be considered statistically different from the dataset.

TABLE 1
Body weights, plasma glucose, and glycated hemoglobin (HbA_{1c}) of treatment groups

	Body weight (g)	Blood glucose (mmol/l)	HbA_{1c} (%)
n	10–13	10–13	9–10
Control	770.9 ± 57.9*	8.24 ± 0.89*	4.39 ± 0.28*
Diabetic	415.8 ± 33.9**	30.95 ± 2.71**	11.69 ± 0.97**
Diabetic + insulin	519.1 ± 42.0	14.81 ± 4.95	8.59 ± 1.17

Values are means ± SD. Starting weights for the groups were 293 ± 8.8 g (mean ± SD; $n = 38$). Nonfasting blood sugar concentration was measured using the Accu-Chek Compact Plus glucometer (Roche, Laval, Quebec City, Canada) and blood glycated hemoglobin (HbA_{1c}) levels by the A1CNow + system (Bayer Healthcare, Sunnyvale, CA). *$P < 0.001$ vs. other groups; **$P < 0.001$ vs. diabetic + insulin (one-way ANOVA with Tukey's test).

RESULTS

STZ-diabetic rats did not suffer weight loss during the study, but they showed reduced weight gain after 22 weeks of STZ-diabetes compared with age-matched controls (Table 1). Persistence of diabetes was indicated by elevated nonfasting blood glucose and glycated hemoglobin levels (Table 1). STZ-diabetic rats that received insulin supplementation for the final 4 weeks of a 22-week period of diabetes showed a partial, but statistically significant,

recovery of body weight, blood glucose, and glycated hemoglobin levels.

To quantitatively assess the effect of diabetes and insulin therapy on the mitochondrial proteome of lumbar DRG, we labeled SC16 immortalized Schwann cells with isotopic forms of lysine (K6) and arginine (R10) and isolated labeled mitochondria to serve as internal standards (Fig. 1*A*). We examined the quantitative accuracy of this approach by mixing the K6R10:K0R0 mitochondria in ratios of 0.75:1, 1.5:1, and 3:1. The K6/K0 or R10/R0 ratios for individual peptides were obtained from MaxQuant analysis, and a linear response was observed after plotting the average peptide ratio obtained from each mixture against the known mixing ratio (supplementary Fig. 1 in online appendix 1). A 25% decrease in protein expression was quantifiable. Unlabeled (K0R0) DRG mitochondria from the three treatments were then individually mixed in a 2:1 ratio with the K6R10 mitochondria prior to SDS-PAGE and LTQ-FT MS/MS analysis. From more than 43,600 identified peptides, 12,785 SILAC pairs were sequenced and ~60% identified. After culling out contaminants (n = 30), reverse-decoy hits (n = 13), and proteins identified by only a single unique peptide, we identified 672 proteins, of which 334 (49.6%) were quantified by at least one unique peptide identified in samples from at least two animals (supplementary online Table 1). The median number of quantified ratios for the three treatments was: control (n = 5), diabetic (n = 8), and diabetic + insulin (n = 7). Of the total proteins identified, 206 (30%) were annotated as mitochondrial/glycolytic and 151 were quantified (73%).

To provide a global view of the effect of diabetes and insulin therapy on protein expression, the expression ratios were binned and a frequency distribution assessed (Fig. 1*B*). In general, diabetes had a more pronounced effect on decreasing protein expression. Insulin therapy induced a rightward shift toward normalizing expression and promoted a significant increase in protein expression. Pathway analysis found that the proteins associated with mitochondrial dysfunction, oxidative phosphorylation, and ubiquinone biosynthesis (primarily complex I proteins) were the most significantly over-represented and showed the greatest percentage of proteins that underwent significant downregulation (Table 2). Consistent with the diabetic phenotype, proteins associated with ketone body biology were also over-represented and diabetes increased the expression of succinyl-CoA:3-ketoacid-CoA transferase one (SCOT), which is critical in acetoacetate clearance.

To determine if diabetes and insulin therapy had a distinct effect on mitochondrial versus nonmitochondrial proteins, the expression ratios for each protein were plotted against each treatment (Fig. 1*C*). This analysis indicated that diabetes has little effect on the majority of mitochondrial and nonmitochondrial proteins that were quantified (the region between solid and dotted lines). With rare exception, insulin therapy did not decrease protein expression, but led to a significant increase in the expression of numerous nonmitochondrial proteins (green shading). Enrichment analysis of proteins in this region using the Biological Networks Gene Ontology (BiNGO) plugin of Cytoscape found that the cluster frequency for proteins annotated to the biologic process of translation was 36.1%, a sevenfold enrichment. We also noted a small group of proteins that were significantly increased by diabetes but whose expression was unchanged by insulin (blue shading). BiNGO analysis of this subset of proteins

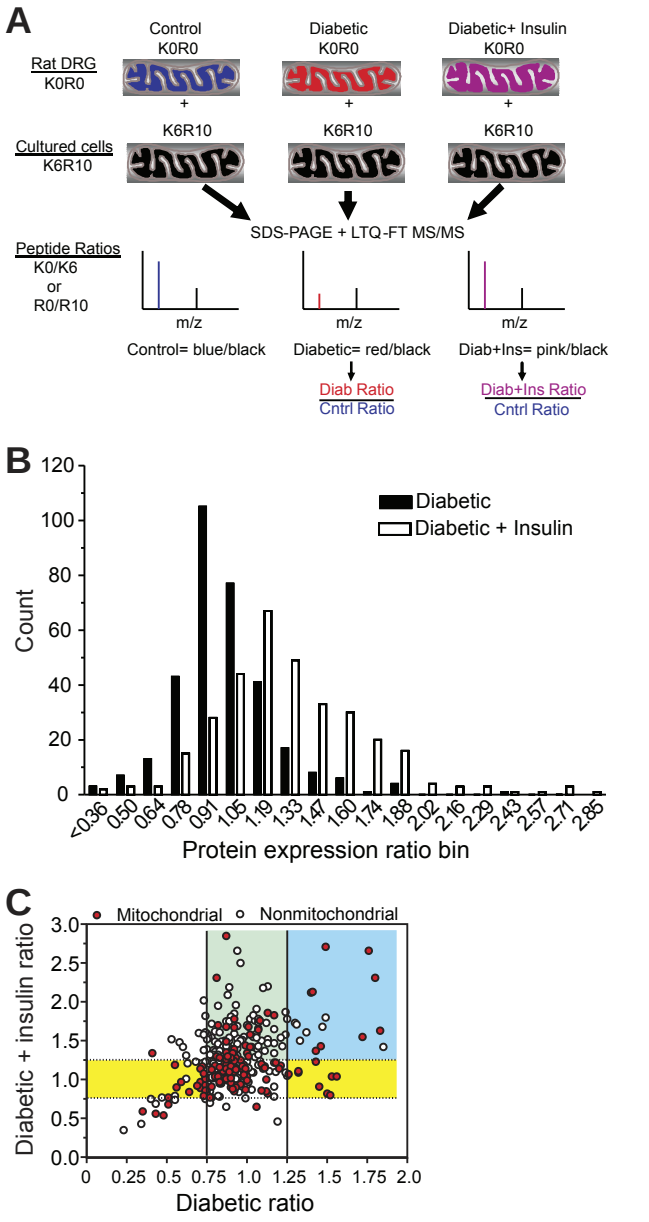

FIG. 1. *A*: Schematic for use of culture-derived isotope tags for quantitative proteomics. Unlabeled (K0R0) mitochondrial fractions were prepared from the lumbar DRGs obtained from each animal in the three treatment groups. Each K0R0 mitochondrial fraction was mixed in a 2:1 ratio with K6R10-labeled mitochondria obtained from SC16 cells that had been metabolically labeled with $^{13}C_6$ lysine (K6) and $^{13}C_6$,$^{15}N_4$ arginine (R10) for 10 days. The proteins were resolved by SDS-PAGE, digested with trypsin, and analyzed by RP-HPLC/LTQ-FT MS/MS. For each protein, the ratio of K0R0 to K6R10 quantifies the endogenous protein relative to the internal standard. Dividing the protein ratios obtained in the diabetic or diabetic + insulin treatment by those obtained from control animals cancels out the K6R10 internal standard and provides the fold control value. *B*: Effect of diabetes and insulin therapy on mitochondrial protein expression. The protein expression ratios from the diabetic and diabetic + insulin treatments were binned and the number of proteins per bin counted. *C*: To determine the effect of diabetes and insulin therapy on mitochondrial versus nonmitochondrial proteins, the expression ratio for each protein was plotted against each treatment. *Solid and dotted lines* demarcate the threshold necessary for proteins to show a significant change in the diabetic and diabetic + insulin treatments, respectively. Proteins in between *dotted and solid lines* did not change with either treatment. Yellow shading indicates proteins that were significantly up- or downregulated by diabetes and normalized by insulin therapy. Blue shading indicates proteins that were increased by diabetes but not normalized by insulin therapy. Green shading indicates proteins not affected by diabetes but increased by insulin therapy.

TABLE 2
Over-represented canonical pathways identified in the proteomic analysis

Canonical pathways	Significance	Ratio, %	Total genes
Mitochondrial dysfunction	3.16×10^{-11}	7.2	171
Oxidative phosphorylation	3.98×10^{-7}	5.4	166
Ubiquinone biosynthesis	7.94×10^{-6}	5.0	119
Methane metabolism	1.25×10^{-4}	4.0	66
Breast cancer regulation by stathmin1	1.59×10^{-4}	4.6	199
Integrin signaling	1.99×10^{-4}	3.5	200
Butanoate metabolism	6.31×10^{-4}	3.0	132
14-3–3-mediated signaling	6.31×10^{-4}	4.4	114
Propanoate metabolism	7.94×10^{-4}	3.1	130
Citrate cycle	7.94×10^{-4}	5.2	58
Valine, leucine and isoleucine degradation	1.00×10^{-3}	3.6	111
Fatty acid metabolism	1.25×10^{-3}	2.6	192
Phenylalanine metabolism	1.25×10^{-3}	2.8	109
Ketone body biology	2.51×10^{-3}	10.5	19
Fatty acid elongation	5.01×10^{-3}	4.4	45
Induction of apoptosis by HIV1	6.31×10^{-3}	4.6	65

Significance provides the confidence of the association as identified by the *P* value of the Fisher exact test. The ratio provides the percentage of proteins associated with the pathway that underwent a significant change. The total genes column refers to all known genes to be linked to the pathway (not necessarily identified by the proteomic screen).

indicated that small G protein signaling and protein transport were the enriched processes.

Diabetes caused a statistically relevant change in 27% of quantified mitochondrial proteins, and insulin therapy had an ameliorative effect that, in general, normalized this decrease (Fig. 1*C*, yellow shading). Consistent with another proteomic study of heart mitochondria (14), bioinformatic analysis found that proteins associated with canonical pathways of mitochondrial dysfunction and oxidative phosphorylation were over-represented and mainly decreased in expression (Table 3). Representative examples from a diabetic animal show a 51% decrease in the complex I protein, NADH dehydrogenase Fe-S protein 3 (NDUFS3) and a 29% decline of Mn superoxide dismutase (Mn-SOD) (Fig. 2*A* and B). However, insulin therapy improved the deficits in NDUFS3 and Mn-SOD expression (Fig. 2*C*) as previously characterized using Western blotting (8,16). On the other hand, diabetes did not alter the expression of ATP synthase α (supplementary Fig. 2 in supplementary online appendix 1).

Lumbar DRG from age-matched control and 22-week-old STZ-diabetic rats were analyzed for rates of oxygen consumption as shown in Fig. 3*A*. Respiratory chain activity, whether coupled or uncoupled, was significantly depressed in diabetic samples. In agreement with the proteomic data and oxygen consumption results, the enzymatic activities of rotenone-sensitive NADH-cytochrome *c* reductase (complex I) and cytochrome *c* oxidase (COX; complex IV), as well as the Krebs cycle enzyme, citrate synthase, were significantly decreased in STZ-diabetic rats compared with control (supplementary Table 2).

Adult sensory neurons were cultured for 1 day from age-matched controls and 22-week-old STZ-diabetic rats and loaded with TMRM. This dye was used at a subquench concentration where a decrease in fluorescence signal intensity indicated reduced mitochondrial inner membrane potential (25). The live neurons were exposed to a combination of antimycin A (inhibitor of complex III) and

TABLE 3
Effect of diabetes and insulin therapy on representative proteins annotated to oxidative phosphorylation and mitochondrial dysfunction

Symbol	Protein description	Fold Control		% Change
		Diabetic	Diabetic + insulin	
ATP5C1	ATP synthase, F1 complex, γ	0.90	1.29*	143
ATP5D	ATP synthase, F1 complex, Δ subunit	0.69*	0.92	133
ATP5F1	ATP synthase, F0 complex, subunit B1	0.92	1.31*	142
ATP5I	ATP synthase, F0 complex, subunit E	0.75*	0.81	108
COX2	Cytochrome c oxidase subunit 2	0.82	1.06	129
COX4I1	Cytochrome c oxidase subunit IV isoform 1¶	0.71*	0.89	125
COX5A	Cytochrome c oxidase subunit Va	0.83	1.28*	154
CPT1A	Carnitine palmitoyltransferase 1A (liver)	0.51*	0.77	172
CYCS	Cytochrome c, somatic	0.56*	0.9	160
HSD17B10	Hydroxysteroid (17-β) dehydrogenase 10	0.71*	1.14	160
ND4	NADH dehydrogenase, subunit 4 (complex I)	0.43*	0.56*	130
NDUFA10	NADH dehydrogenase 1 α subcomplex 10§	0.73*	0.79	108
NDUFA13	NADH dehydrogenase 1 α subcomplex, 13	0.35*	0.59*	168
NDUFB10	NADH dehydrogenase 1 β subcomplex, 10	0.94	1.4*	148
NDUFS1	NADH dehydrogenase Fe-S protein 1	0.78	0.91	116
NDUFS2	NADH dehydrogenase Fe-S protein 2	0.48*	0.54	113
NDUFS3	NADH dehydrogenase Fe-S protein 3¶	0.64*	0.84	131
NDUFS8	NADH dehydrogenase Fe-S protein 8	0.91	1.34*	147
PRDX3	Peroxiredoxin 3	0.87	1.26*	145
PRDX5	Peroxiredoxin 5	0.74*	0.86	116
SOD2	Superoxide dismutase 2, mitochondrial¶	0.73*	1.08	148
UQCRC1	Ubiquinol-cytochrome c reductase I	0.87	1.26*	145

Values shown are the mean and the asterisk (*) indicates proteins that showed a significant change in expression. Percent change represents effect of insulin treatment on the protein expression ratio measured from diabetic rats. Please see online supplementary Table 1 for more complete information. ¶Confirming references (8,16); §Confirming reference (29).

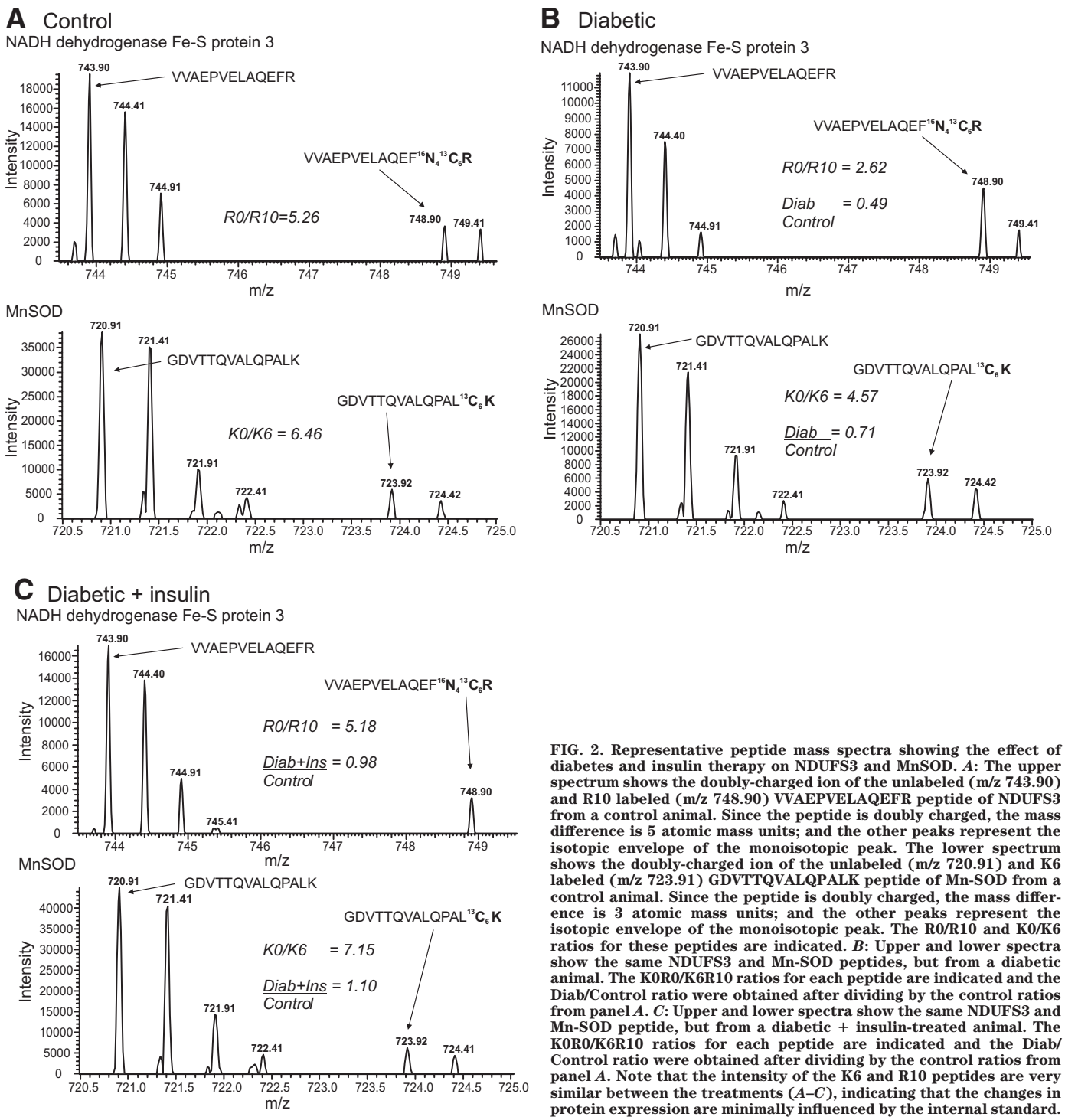

FIG. 2. Representative peptide mass spectra showing the effect of diabetes and insulin therapy on NDUFS3 and MnSOD. *A*: The upper spectrum shows the doubly-charged ion of the unlabeled (m/z 743.90) and R10 labeled (m/z 748.90) VVAEPVELAQEFR peptide of NDUFS3 from a control animal. Since the peptide is doubly charged, the mass difference is 5 atomic mass units; and the other peaks represent the isotopic envelope of the monoisotopic peak. The lower spectrum shows the doubly-charged ion of the unlabeled (m/z 720.91) and K6 labeled (m/z 723.91) GDVTTQVALQPALK peptide of Mn-SOD from a control animal. Since the peptide is doubly charged, the mass difference is 3 atomic mass units; and the other peaks represent the isotopic envelope of the monoisotopic peak. The R0/R10 and K0/K6 ratios for these peptides are indicated. *B*: Upper and lower spectra show the same NDUFS3 and Mn-SOD peptides, but from a diabetic animal. The K0R0/K6R10 ratios for each peptide are indicated and the Diab/Control ratio were obtained after dividing by the control ratios from panel *A*. *C*: Upper and lower spectra show the same NDUFS3 and Mn-SOD peptide, but from a diabetic + insulin-treated animal. The K0R0/K6R10 ratios for each peptide are indicated and the Diab/Control ratio were obtained after dividing by the control ratios from panel *A*. Note that the intensity of the K6 and R10 peptides are very similar between the treatments (*A–C*), indicating that the changes in protein expression are minimally influenced by the internal standard.

oligomycin (inhibitor of ATP synthase), and the fluorescence signal in axons detected by confocal microscopy. Antimycin A blocks electron transfer leading to mitochondrial depolarization, whereas oligomycin inhibits the ATPase and prevents reverse pumping of protons and associated generation of a proton gradient. Therefore, the mitochondrial membrane potential (and associated proton gradient) is completely dissipated in the presence of both these drugs. In the presence of antimycin A + oligomycin, the rate of mitochondrial depolarization was more rapid in axons of normal neurons compared with diabetic neurons (Fig. 3*B–D*). This suggests that prior to the addition of antimycin A + oligomycin, the axonal mitochondria were more highly polarized in the normal neurons compared with the diabetic neurons. Mitochondrial physiology was further investigated by treating cultured neurons from control and diabetic rats with oligomycin alone. Blockade of the ATPase results in a buildup of the transmembrane proton gradient and induces hyperpolarization of the mitochondrial inner membrane, as indicated by elevated TMRM fluorescence (Fig. 4*A*) (26). In normal neurons, a transient hyperpolarization was observed, followed by a recovery due to adaption of the respiratory chain. For example, uncoupling proteins become active and dissipate the proton gradient under a high inner membrane potential (27). Diabetic neurons exhibited a significantly greater

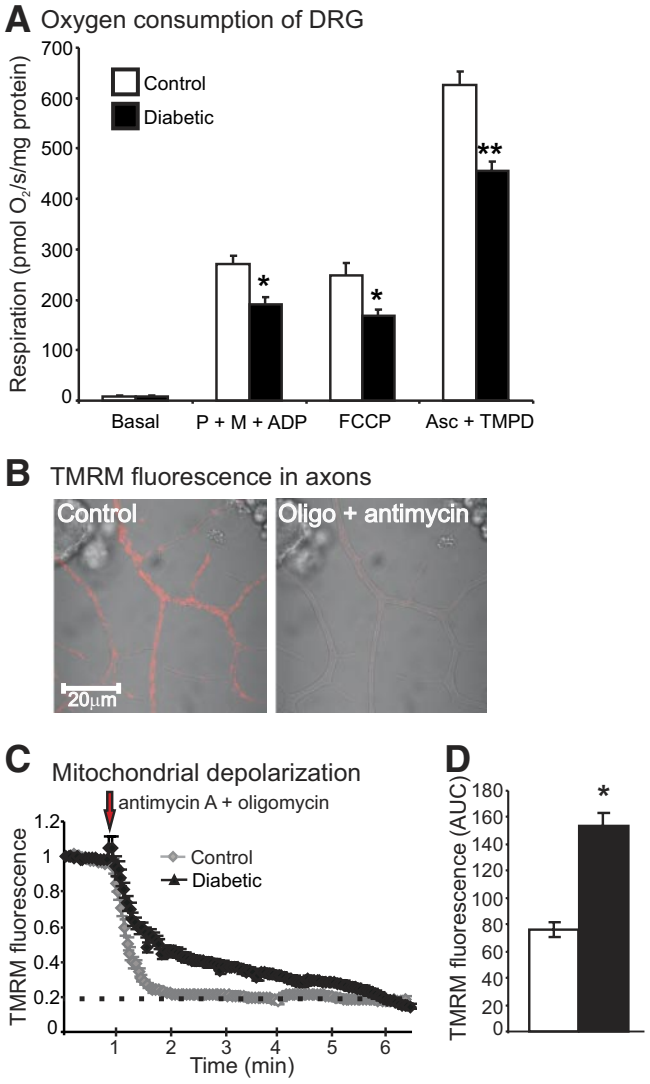

FIG. 3. The mitochondria of DRG sensory neurons exhibited lower respiratory chain activity. *A*: Oxygen consumption was assessed in freshly isolated mitochondria from lumbar DRG of age-matched control and 22-week-old diabetic rats using an OROBOROS oxygraph 2k. Coupled respiration rates were measured in the presence of pyruvate (P) (10 mmol/l), malate (M) (5.0 mmol/l), and ADP (2.0 mmol/l). The addition of FCCP (0.5 μmol/l) permits a measure of uncoupled respiratory chain activity. Addition of ascorbate (Asc) (5.0 mmol/l) and TMPD (0.5 mmol/l) permit an analysis of complex IV activity that was verified by specific inhibitors. Values are mean ± SEM; $n = 5$. *$P < 0.05$ vs. controls; **$P < 0.001$ vs. controls. *B*: Images of fluorescence confocal microscopy using TMRM in live cultures of DRG neurons isolated from control adult rats showing effect of antimycin A and oligomycin. *C*: Trace of TMRM fluorescence signal in the axons of cultured DRG neurons isolated from age-matched controls and STZ-diabetic rats. *D*: Shows the area under the TMRM fluorescence trace (area under the curve) for control (*open bar*) and diabetic (*filled bar*) neurons. The area under the curve was estimated from the baseline (at the point of injection) to a fluorescence level of 0.2 and between time points 1.0 min and 6 min using sums of squares (shown by *dotted line*). Values are the means ± SEM, $n = 65–80$ axons; *$P < 0.001$ compared with control, *t* test. The TMRM trace was characterized by nonlinear regression (one phase exponential decay). The rate constant of decay (K) = 0.013 ± 0.0004 (control) and 0.006 ± 0.0001 (diabetic). Half-life of decay = 54.19 s (control) and 108.7 s (diabetic). The Fisher parametric (F) ratio = 409.5, $P < 0.0001$, control vs. diabetic. The F ratio compares the goodness-of-fit of the two curves. The *red arrow* indicates point of injection of antimycin A + oligomycin. (A high-quality digital representation of this figure is available in the online issue.)

level of hyperpolarization upon oligomycin application and the adaptive response was impaired.

We determined if the respiratory chain was contributing to oxidative stress in diabetic neurons by loading cells with the mitochondrially-targeted ROS detector, MitoSOX red. A subset of diabetic neurons was pretreated with oligomycin to hyperpolarize the inner mitochondrial membrane and maximize loading of MitoSOX red into the mitochondrial matrix. Neurons were treated with the uncoupler, carbonylcyanide-p-trifluoromethoxyphenylhydrazone (FCCP), to dissipate the transmembrane electrochemical gradient and enhance the rate of electron transfer. Increased respiratory chain activity leads to augmented electron leakage and associated generation of ROS, primarily superoxide. In normal neurons this was demonstrated with elevated FCCP-induced MitoSOX red fluorescence (Fig. 4*F* and *G*). Diabetic neurons, with or without prior oligomycin treatment, exhibited lower MitoSOX red fluorescence intensities indicative of reduced levels of superoxide being generated by the respiratory chain.

Parallel cultures demonstrated elevated oxidative stress in axons of diabetic neurons under 25 mmol/l glucose versus control neurons as exhibited by raised dichlorodihydrofluorescein (DCF) fluorescence and enhanced staining for adducts of 4-HNE (Fig. 5*A–F*). Subsets of these cultures were treated acutely with the specific SDH inhibitor, SDI-158, to investigate the role of the polyol pathway in ROS production. Figure 5*G* and *H* shows that blockade of high glucose-dependent sorbitol production results in reduced ROS generation in axons of diabetic neurons.

DISCUSSION

The results show that respiratory chain components of the mitochondrial proteome are downregulated in DRG in diabetes and this phenotypic alteration was associated with impairment in respiratory chain activity. In addition, for the first time, this study demonstrates that altered mitochondrial proteome expression is linked to altered mitochondrial physiology in axons of diabetic neurons. And finally, although oxidative stress was present in axons of diabetic neurons, the results show that polyol pathway activity, not aberrant respiratory chain function, contributes to generation of ROS.

We used SILAC to provide a set of culture-derived isotope tags (20) to serve as internal standards for quantifying the effect of diabetes on the composition of the mitochondrial proteome from DRG. One advantage of culture-derived isotope tags is the quantitative accuracy that can be achieved relative to label-free approaches (28), especially for low abundant proteins. Despite our small sample size, a 25% change in expression was sufficient to reach statistical significance, and the number of mitochondrial proteins that exceeded this threshold was similar to that previously reported in mitochondria isolated from heart tissue of diabetic Akita mice (14). Further, the results of our unbiased quantification were in close agreement with those obtained by targeted immunoblot analyses for COX subunit IV, NDUFS3, ATP synthase, and Mn-SOD in two prior studies (8,16).

Similar to a previous gene array study delineating alterations in mRNA expression in DRG from diabetic rats (29), the magnitude of changes observed in the mitochondrial proteins were rather modest and averaged 0.44 ± 0.16-fold in either direction. Interestingly, the gene array study

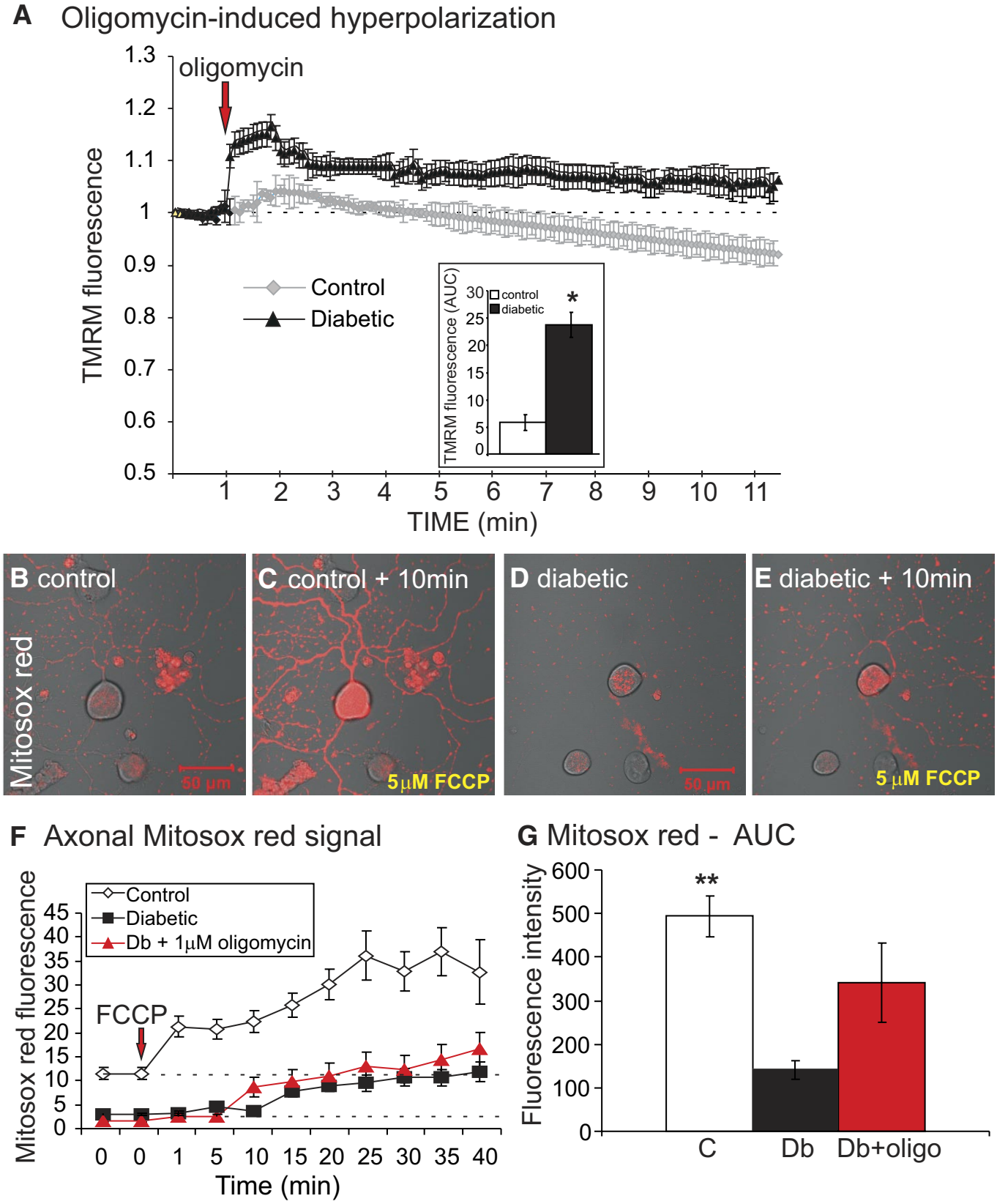

FIG. 4. Impaired respiratory function is associated with reduced ROS generation in the mitochondrial matrix of cultured neurons isolated from STZ-diabetic rats. *A*: TMRM fluorescence trace of oligomycin-induced mitochondrial inner membrane hyperpolarization in the axons of control and diabetic neurons. Values are mean ± SEM, n = 65–85 axons. Inset shows the area under the TMRM fluorescence trace (AUC) for control (open bar) and diabetic (filled bar) neurons. The AUC was estimated from the baseline (at the point of injection, dotted line), and between time points of 1.0 min and 4 min using sums of squares. Values are mean ± SEM, n = 65–80 axons,*$P < 0.01$ compared with control, t test. The *red arrow* indicates point of injection of oligomycin. *B–E*: Images of MitoSOX red fluorescence in cultures of DRG neurons showing the effect of 5.0 μmol/l FCCP. *F*: Quantification of real-time MitoSOX red fluorescence levels in the axons of cultured DRG neurons after 5.0 μmol/l FCCP

Continued on facing page

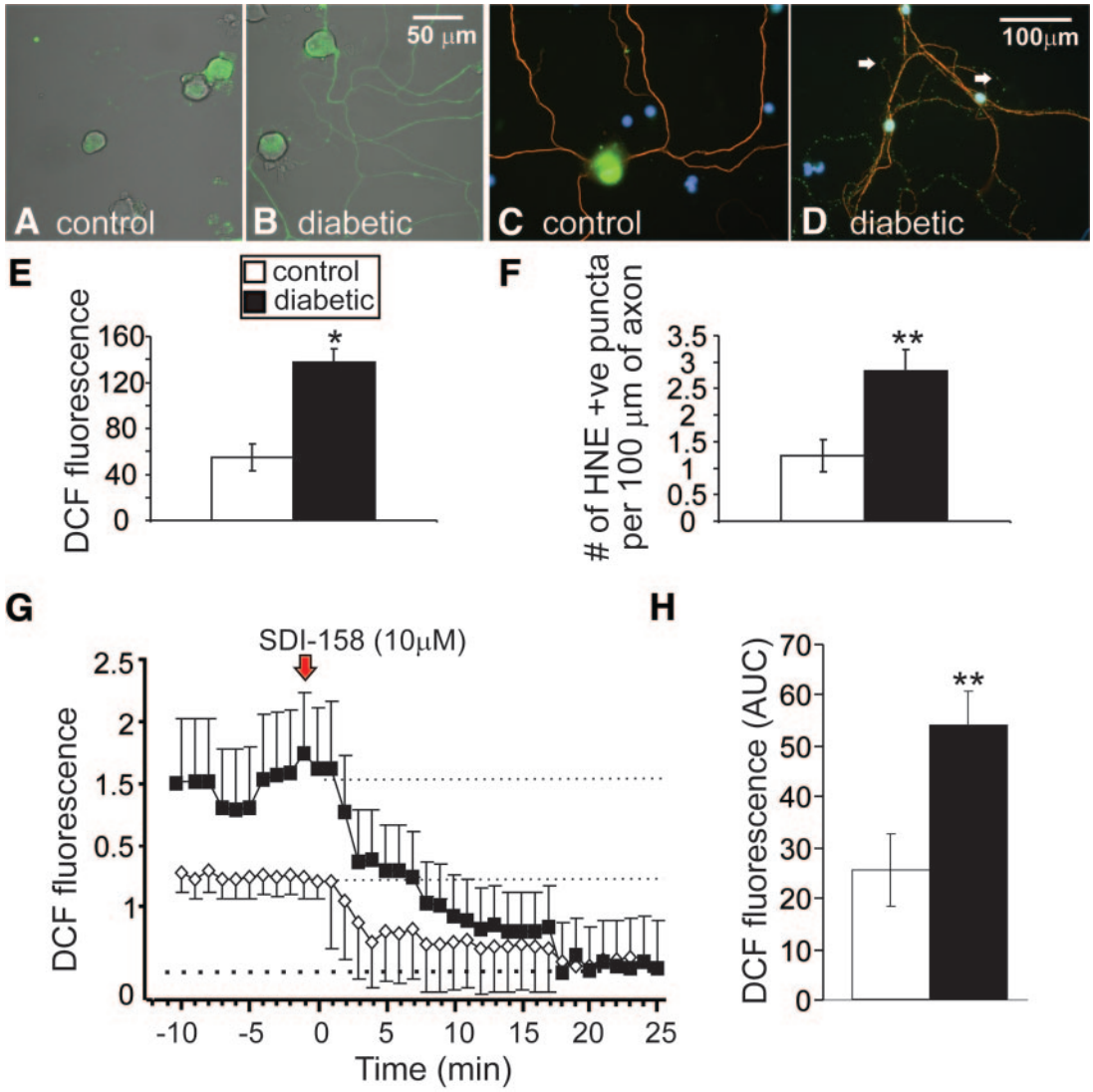

FIG. 5. Axons of sensory neurons from STZ-diabetic rats exhibit elevated oxidative stress that is ameliorated by the blockade of SDH. Images of ROS levels in axons at 24 h in adult DRG neuron culture from (*A*) control and (*B*) STZ-diabetic rats. Cultures were stained for ROS using CM-H_2DCFDA dye (DCF is the fluorescent product resulting from oxidation). *E*: Quantification of ROS accumulation in axons. Values are means ± SEM, n = 44–57 axons, *P < 0.05 by t test. Immunofluorescent images of accumulation of adducts of 4-HNE in axons in sensory neuron cultures after 3 days; (*C*) is control and (*D*) is diabetic culture. *F*: Level of accumulation of puncta of adducts of 4-HNE in axons. Values are means ± SEM, n = 19–27 axons, **P < 0.01 by t test. *G*: Trace of DCF-fluorescence signal in the axons of cultured DRG neurons isolated from age-matched controls and STZ-diabetic rats and treated acutely with 10 μmol/l SDI-158. DCF fluorescence trace was characterized by nonlinear regression (one phase exponential decay). K = 0.09 ± 0.02 (control) and 0.13 ± 0.009 (diabetic). Half-life of decay = 7.5 min (control) and 5.5 min (diabetic). F ratio = 50.33, P < 0.0001, control versus diabetic. The *red arrow* indicates point of injection of SDI-158. *H* shows the area under the DCF fluorescence trace (AUC) for control (*open bar*) and diabetic (*filled bar*) neurons. The AUC was estimated from 0.2 to 1.6 on fluorescence axis and between time points 0 to 22 min using sums of squares (*dotted lines* show upper and lower limits). Values are means ± SEM, n = 42–51 axons; **P < 0.01 compared with control by t test. (A high-quality digital representation of this figure is available in the online issue.)

reported that after 2 months of diabetes, no modification occurred in gene expression of enzymes associated with the tricarboxylic acid cycle. We also observed no changes in pyruvate dehydrogenase and in six of eight of the tricarboxylic acid cycle enzymes at the protein level, the exceptions being fumarate hydratase and succinyl Co-A ligase. Similarly, with the exception of hexokinase 1, the remaining glycolytic enzymes were not altered, in agreement with mRNA expression studies at 2 months of diabetes (29). We previously reported that hexokinase 1 localizes to mitochondria of DRG (30) and this protein was reproducibly detected in the heavy mitochondrial fraction of all animals. Interestingly, although the hexokinase gene and protein expression were not modified after 2–3 months of diabetes in two studies (29–30), expression was decreased after 22 weeks of diabetes in the present study. Since this was the only glycolytic enzyme that significantly changed, it is tempting to speculate that its lowered expression also has a function separate from glucose metabolism. In this regard, sensory neurons from diabetic adult animals have an impaired ability to support neurite

treatment. MitoSOX trace was characterized by nonlinear regression. F ratio = 32.48, P < 0.0001 (control vs. diabetic with or without oligomycin by one-way ANOVA). Values are mean ± SEM, n = 18–73 axons. *G*: Area under the curve for MitoSOX red fluorescence intensity levels. Values are mean ± SEM, n = 35–73 axons; **P < 0.001 compared with diabetic or diabetic + oligomycin-treated cells by one-way ANOVA. (A high-quality digital representation of this figure is available in the online issue.)

development (16) and directly inhibiting hexokinase activity blocks neurotrophin-induced neuritogenesis (31).

In the cardiac system, diminished mitochondrial respiratory function caused by diabetes has also been identified by proteomic and gene array techniques (14,32). These broad changes in gene expression could be triggered by altered activity of key upstream regulators. For example, in human skeletal muscle in type 2 diabetes, the transcriptional regulator NRF-1 and the transcriptional coactivator peroxisome proliferator-activated receptor-γ coactivator 1 α (PGC-1α) were downregulated and corresponded with reduced expression of proteins that regulate cellular energy metabolism, including mitochondrial biogenesis and oxidative phosphorylation (33,34). In fact, our preliminary data demonstrated a significant reduction in activity of AMP kinase, a regulator of PGC1-α, in DRG in type 1 diabetic rodents (manuscript in preparation).

Initial exposure to high glucose concentration over 1 to 4 weeks in DRG in diabetic rats is linked to upregulation of glycolytic pathway expression (mRNA) (29). Studies in endothelial or Schwann cells demonstrate that acute exposure to glucose elevates ROS and respiratory chain activity, respectively (2,23). Therefore, in the short term, hyperglycemia triggers enhanced glycolysis and associated respiratory chain activity (and possibly ROS). However, in the longer term, the high intracellular glucose concentration provides an ample supply of ATP via several nonmitochondrial-dependent pathways. Consequently, the metabolic phenotype of the cell adapts and functions in the absence of a dependence on the tricarboxylic acid cycle and oxidative phosphorylation for ATP production, possibly by initiating a process homologous to the "Crabtree effect" (35). Thus, rates of electron donation to the respiratory chain are suboptimal in neurons in long-term diabetic rats and may predispose to lower rates of mitochondrial respiratory chain activity and oxidative phosphorylation. Key metabolic activity sensors and/or regulators such as AMPK and NRF-1 are putative candidates for this modulation, although it is unlikely that subsequently adapted metabolism of glucose is channeled through glycolysis in isolation. In this regard, elevated glucose flux through the aldehyde and aldose reductase pathway could be critical (24,36). For example, studies in lens (37), retina (5), and cardiac tissue (38) in medium- to long-term animal models of type 1 diabetes show that parts of the glycolytic pathway function are depressed.

ROS production linked to enhanced electron leakage from the respiratory chain induced by uncoupling, and theoretically comprising superoxide, was lower in the axons of neurons from diabetic rats (Fig. 4*B–E*), confirming our mitochondrial physiology and proteomics work. This was also in spite of generally elevated ROS levels in axons (Fig. 5*A–F*). The studies in Figs. 4 and 5*G* provide preliminary evidence that the sources of ROS in axons of diabetic neurons are not from aberrant respiratory chain function, but in part from polyol pathway activity. The latter pathway has been proposed as a source of ROS through a putative sorbitol accumulation-dependent NADPH oxidase route in previous studies (24,36). Downregulation of the respiratory chain machinery would be predicted to lead to depolarization of the mitochondrial membrane (Fig. 3*B–D*), reduced rates of respiratory chain activity (8) (Fig. 3*A* and supplementary Table 2), and associated diminished electron leakage. The lower rate of loss of polarization status subsequent to uncoupling in Fig. 3*C* was not the result of resistance to uncoupling in the diabetic neurons since complementary measures of respiratory chain activity show lower rates of electron transfer in diabetic neurons; also, see Fig. 1 in Chowdhury et al. (8). These findings differ from those in cultured endothelial cells where high glucose concentration enhanced mitochondrial membrane potential and induced elevated ROS (2–3). Figure 4*A* reveals that oligomycin treatment caused a greater level of mitochondrial inner membrane hyperpolarization above baseline in diabetic neurons compared with normal neurons, further highlighting that adult sensory neurons with a history of diabetes and under high glucose concentration behave differently to endothelial cells. The adaption of mitochondria in normal neurons to hyperpolarization was not observed in diabetic neurons, again stressing the aberrant phenotype of mitochondrial physiology. Uncoupling proteins such as adenine nucleotide transporters (ANT1/2) contribute to the dissipation of a high mitochondrial membrane potential (27) and expression was depressed in diabetic mitochondria (supplementary Table 1).

In conclusion, our proteomics data reveal a range of altered expression profiles in the mitochondrial proteome of DRG from diabetic rats. This modified expression pattern was associated with aberrant mitochondrial respiratory chain physiology and function. Under high glucose concentration, the neuron cell body perceives that mitochondrial function can be downgraded; however, this may ignore the unique high-energy requirements of the nerve ending and contribute to distal axon degeneration. For example, growth cone motility that underpins axonal plasticity and regeneration in the skin has an exceedingly high demand for ATP because of significant levels of actin treadmilling (39). Impaired respiratory chain function did not elevate ROS generation, even though oxidative stress was observed in axons. In fact, the lower rates of respiratory chain activity were linked to mitochondrial membrane depolarization, improper adaption to oligomycin-induced membrane hyperpolarization, and reduced levels of superoxide derived from electron leakage during electron transport. In axons of neurons from long-term diabetic rats, sites of ROS production colocalize with the mitochondrial compartment (16,40). Therefore, alternative mitochondrial-related sources of ROS should be considered. For example, NADPH oxidase has been localized to the mitochondrial compartment of kidney cortex and mesanglial cells and mediates elevated ROS under high glucose concentration (41).

ACKNOWLEDGMENTS

This work was supported by grants from the Juvenile Diabetes Research Foundation (#1-2008-280) and the National Institutes of Health to R.T.D. (grants NS-054847 and DK-073594). E.A. was supported by a grant from the National Science and Engineering Research Council (#3311686-06) to P.F. and subsequently by a postgraduate scholarship from the Manitoba Health Research Council. S.K.R.C. and E.Z. were supported by grants to P.F. from the Canadian Institutes for Health Research (#MOP-84214) and the Juvenile Diabetes Research Foundation (#1-2008-193). D.R.S. was supported by a grant to P.F. from the Manitoba Health Research Council. This work was also funded by the St. Boniface General Hospital and Research Foundation.

No potential conflicts of interest relevant to this article were reported.

E.A. and E.Z. contributed equally to the fluorescence imaging experiments described in Figs. 3–5. E.A. performed preparation of mitochondrial samples for proteomic analysis. S.K.R.C. performed the mitochondrial respiration and complex activity studies. D.R.S. was responsible for induction of diabetes and maintenance of all animal groups, analysis of blood glucose/glycated hemoglobin, and dissection of DRG for mitochondrial measurements. R.T.D. designed and performed the proteomic analysis and contributed to writing and editing the manuscript. P.F. designed the animal and tissue culture studies and contributed to writing and editing of the manuscript.

The authors thank Dr. Gordon Glazner, University of Manitoba, and St. Boniface Hospital Research Centre for permitting access to the Carl Zeiss LSM 510.

REFERENCES

1. Vincent AM, Russell JW, Low P, Feldman EL. Oxidative stress in the pathogenesis of diabetic neuropathy. Endocr Rev 2004;25:612–628
2. Nishikawa T, Edelstein D, Du XL, Yamagishi S, Matsumura T, Kaneda Y, Yorek MA, Beebe D, Oates PJ, Hammes HP, Giardino I, Brownlee M. Normalizing mitochondrial superoxide production blocks three pathways of hyperglycaemic damage. Nature 2000;404:787–790
3. Du XL, Edelstein D, Rossetti L, Fantus IG, Goldberg H, Ziyadeh F, Wu J, Brownlee M. Hyperglycemia-induced mitochondrial superoxide overproduction activates the hexosamine pathway and induces plasminogen activator inhibitor-1 expression by increasing Sp1 glycosylation. Proc Natl Acad Sci U S A 2000;97:12222–12226
4. Coppey LJ, Gellett JS, Davidson EP, Yorek MA. Preventing superoxide formation in epineurial arterioles of the sciatic nerve from diabetic rats restores endothelium-dependent vasodilation. Free Radic Res 2003;37:33–40
5. Ola MS, Berkich DA, Xu Y, King MT, Gardner TW, Simpson I, LaNoue KF. Analysis of glucose metabolism in diabetic rat retinas. Am J Physiol Endocrinol Metab 2006;290:E1057–1067
6. Huang TJ, Price SA, Chilton L, Calcutt NA, Tomlinson DR, Verkhratsky A, Fernyhough P. Insulin prevents depolarization of the mitochondrial inner membrane in sensory neurons of type 1 diabetic rats in the presence of sustained hyperglycemia. Diabetes 2003;52:2129–2136
7. Srinivasan S, Stevens M, Wiley JW. Diabetic peripheral neuropathy: evidence for apoptosis and associated mitochondrial dysfunction. Diabetes 2000;49:1932–1938
8. Chowdhury SK, Zherebitskaya E, Smith DR, Akude E, Chattopadhyay S, Jolivalt CG, Calcutt NA, Fernyhough P. Mitochondrial respiratory chain dysfunction in dorsal root ganglia of streptozotocin-induced diabetic rats and its correction by insulin treatment. Diabetes 2010;59:1082–1091
9. Lashin OM, Szweda PA, Szweda LI, Romani AM. Decreased complex II respiration and HNE-modified SDH subunit in diabetic heart. Free Radic Biol Med 2006;40:886–896
10. Yang JY, Yeh HY, Lin K, Wang PH. Insulin stimulates Akt translocation to mitochondria: implications on dysregulation of mitochondrial oxidative phosphorylation in diabetic myocardium. J Mol Cell Cardiol 2009;46:919–926
11. Kelley DE, He J, Menshikova EV, Ritov VB. Dysfunction of mitochondria in human skeletal muscle in type 2 diabetes. Diabetes 2002;51:2944–2950
12. Kruszynska YT, Mulford MI, Baloga J, Yu JG, Olefsky JM. Regulation of skeletal muscle hexokinase II by insulin in nondiabetic and NIDDM subjects. Diabetes 1998;47:1107–1113
13. Mogensen M, Sahlin K, Fernstrom M, Glintborg D, Vind BF, Beck-Nielsen H, Hojlund K. Mitochondrial respiration is decreased in skeletal muscle of patients with type 2 diabetes. Diabetes 2007;56:1592–1599
14. Bugger H, Chen D, Riehle C, Soto J, Theobald HA, Hu XX, Ganesan B, Weimer BC, Abel ED. Tissue-specific remodeling of the mitochondrial proteome in type 1 diabetic akita mice. Diabetes 2009;58:1986–1997
15. Tomlinson DR, Gardiner NJ. Glucose neurotoxicity. Nat Rev Neurosci 2008;9:36–45
16. Zherebitskaya E, Akude E, Smith DR, Fernyhough P. Development of selective axonopathy in adult sensory neurons isolated from diabetic rats: role of glucose-induced oxidative stress. Diabetes 2009;58:1356–1364
17. Kennedy WR, Wendelschafer-Crabb G, Johnson T. Quantitation of epidermal nerves in diabetic neuropathy. Neurology 1996;47:1042–1048
18. Polydefkis M, Hauer P, Sheth S, Sirdofsky M, Griffin JW, McArthur JC. The time course of epidermal nerve fibre regeneration: studies in normal controls and in people with diabetes, with and without neuropathy. Brain 2004;127:1606–1615
19. Ong SE, Blagoev B, Kratchmarova I, Kristensen DB, Steen H, Pandey A, Mann M. Stable isotope labeling by amino acids in cell culture, SILAC, as a simple and accurate approach to expression proteomics. MolCell Proteomics 2002;1:376–386
20. Ishihama Y, Sato T, Tabata T, Miyamoto N, Sagane K, Nagasu T, Oda Y. Quantitative mouse brain proteomics using culture-derived isotope tags as internal standards. Nat Biotechnol 2005;23:617–621
21. Frezza C, Cipolat S, Scorrano L. Organelle isolation: functional mitochondria from mouse liver, muscle and cultured fibroblasts. Nat Protoc 2007;2:287–295
22. Yu C, Alterman M, Dobrowsky RT. Ceramide displaces cholesterol from lipid rafts and decreases the association of the cholesterol binding protein caveolin-1. J Lipid Res 2005;46:1678–1691
23. Zhang L, Yu C, Vasquez FE, Galeva N, Onyango I, Swerdlow RH, Dobrowsky RT. Hyperglycemia alters the Schwann cell mitochondrial proteome and decreases coupled respiration in the absence of superoxide production. J Proteome Res 2010;9:458–471
24. Oates PJ. Aldose reductase, still a compelling target for diabetic neuropathy. Curr Drug Targets 2008;9:14–36
25. Nicholls DG. Simultaneous monitoring of ionophore- and inhibitor-mediated plasma and mitochondrial membrane potential changes in cultured neurons. J Biol Chem 2006;281:14864–14874
26. Jekabsons MB, Nicholls DG. In situ respiration and bioenergetic status of mitochondria in primary cerebellar granule neuronal cultures exposed continuously to glutamate. J Biol Chem 2004;279:32989–33000
27. Azzu V, Parker N, Brand MD. High membrane potential promotes alkenal-induced mitochondrial uncoupling and influences adenine nucleotide translocase conformation. Biochem J 2008;413:323–332
28. Geiger T, Cox J, Ostasiewicz P, Wisniewski JR, Mann M. Super-SILAC mix for quantitative proteomics of human tumor tissue. Nat Methods. 2010;7:383–385
29. Price SA, Zeef LA, Wardleworth L, Hayes A, Tomlinson DR. Identification of changes in gene expression in dorsal root ganglia in diabetic neuropathy: correlation with functional deficits. J Neuropathol Exp Neurol 2006;65:722–732
30. Gardiner NJ, Wang Z, Luke C, Gott A, Price SA, Fernyhough P. Expression of hexokinase isoforms in the dorsal root ganglion of the adult rat and effect of experimental diabetes. Brain Res 2007;1175:143–154
31. Wang Z, Gardiner NJ, Fernyhough P. Blockade of hexokinase activity and binding to mitochondria inhibits neurite outgrowth in cultured adult rat sensory neurons. Neurosci Lett 2008;434:6–11
32. Bugger H, Abel ED. Molecular mechanisms for myocardial mitochondrial dysfunction in the metabolic syndrome. Clin Sci (Lond) 2008;114:195–210
33. Mootha VK, Lindgren CM, Eriksson KF, Subramanian A, Sihag S, Lehar J, Puigserver P, Carlsson E, Ridderstrale M, Laurila E, Houstis N, Daly MJ, Patterson N, Mesirov JP, Golub TR, Tamayo P, Spiegelman B, Lander ES, Hirschhorn JN, Altshuler D, Groop LC. PGC-1alpha-responsive genes involved in oxidative phosphorylation are coordinately downregulated in human diabetes. Nat Genet 2003;34:267–273
34. Patti ME, Butte AJ, Crunkhorn S, Cusi K, Berria R, Kashyap S, Miyazaki Y, Kohane I, Costello M, Saccone R, Landaker EJ, Goldfine AB, Mun E, DeFronzo R, Finlayson J, Kahn CR, Mandarino LJ. Coordinated reduction of genes of oxidative metabolism in humans with insulin resistance and diabetes: potential role of PGC1 and NRF1. Proc Natl Acad Sci U S A 2003;100:8466–8471
35. Ibsen HK. The Crabtree effect: a review. Cancer Res 1961;21:829–841
36. Ido Y, Nyengaard JR, Chang K, Tilton RG, Kilo C, Mylari BL, Oates PJ, Williamson JR. Early neural and vascular dysfunctions in diabetic rats are largely sequelae of increased sorbitol oxidation. Antioxid Redox Signal 2010;12:39–51
37. Obrosova I, Faller A, Burgan J, Ostrow E, Williamson JR. Glycolytic pathway, redox state of NAD(P)-couples and energy metabolism in lens in galactose-fed rats: effect of an aldose reductase inhibitor. Curr Eye Res 1997;16:34–43
38. Trueblood N, Ramasamy R. Aldose reductase inhibition improves altered glucose metabolism of isolated diabetic rat hearts. Am J Physiol 1998;275:H75–83
39. Bernstein BW, Bamburg JR. Actin-ATP hydrolysis is a major energy drain for neurons. J Neurosci 2003;23:1–6
40. Akude E, Zherebitskaya E, Roy Chowdhury SK, Girling K, Fernyhough P. 4-Hydroxy-2-nonenal induces mitochondrial dysfunction and aberrant axonal outgrowth in adult sensory neurons that mimics features of diabetic neuropathy. Neurotox Res 2010;17:28–38
41. Block K, Gorin Y, Abboud HE. Subcellular localization of Nox4 and regulation in diabetes. Proc Natl Acad Sci U S A 2009;106:14385–14390